



# Unmodified silver nanoparticles for dual detection of dithiocarbamate fungicide and rapid degradation of water pollutants

P. N. Ragam<sup>1</sup> · B. Mathew<sup>1</sup>

Received: 11 December 2018 / Revised: 8 May 2019 / Accepted: 24 June 2019 / Published online: 1 July 2019  
© Islamic Azad University (IAU) 2019

## Abstract

Herein, for the first time, any phytochemical-based silver nanoparticle is reported as a dual sensor to detect toxic dithiocarbamate fungicide (Thiram) spectrophotometrically and electrochemically. Green approach was employed for the silver nanoparticle synthesis utilizing the stem extract of *Coscinium fenestratum* via a microwave-assisted route. The characterization of silver nanoparticles was carried out by methods such as UV–visible, Fourier transform-infrared, and X-ray diffraction spectroscopy, as well as transmission electron microscopy techniques. The diffraction and microscopic studies proved that the nanoparticles were essentially crystalline and almost spherically shaped with average size of  $20.72 \pm 4.25$  nm. The nanoparticles were found very stable for more than 6 months and hence are appropriate for remediation of several issues regarding environment such as detection of fungicide as well as organic dye degradation. Thus, the nanoparticles were explored for selective recognition of Thiram and obtained a low limit of detection of 0.18 ppm, much lower than 7 ppm, the maximal residue limit as per the environmental protection agency of the USA. Moreover, the nanoparticles successfully detected Thiram from real samples from tap, canal, and river water in the state of Kerala, India. Furthermore, the nanoparticles were utilized for their excellent catalytic efficiency toward the swift degradation of three water contaminant organic dyes, namely methylene blue, methyl orange, and naphthol green B within a couple of minutes.

**Keywords** Dye degradation · Electrochemical sensing · Optical sensing · Silver nanoparticles · Thiram

## Introduction

Tetramethylthiuram disulfide or Thiram is one of the most renowned dithiocarbamates used worldwide in rubber processing, as fungicide and animal repellent (Hasan 2010). It is a noted allergen which induces the excess release of histamine in humans leading to headache, digestive problems, nausea, elevation of blood pressure, vomiting, and so forth (Rouabhi 2010). Moreover, Thiram is observed to inactivate glutathione reductase enzyme which can increase oxidative stress in human cells as a result of the accumulation

of dangerous free radicals (Cereser et al. 2001). It is also known as a mutagen, inducing variation in chromosomes (Slimani et al. 2018; Paschin and Bakhitova 1985). From industrial wastes and agricultural fields, Thiram directly pollutes the environment and eventually affects aquatic beings, birds, and humans creating severe health impacts. Hence, monitoring Thiram in the environment is exceedingly relevant (Rouabhi 2010). Recently, several reports on the recognition of Thiram utilized surface-enhanced Raman spectroscopy (SERS), fluorescence spectroscopy, colorimetry, cyclic and square wave voltammetry, and HPLC. However, one can see that the materials used in such cases employ toxic chemicals during their synthesis and thus not safe in practical applications (Rohit and Kailasa 2014; Wang et al. 2015; Yang et al. 2014; Fei Chan et al. 2013; Yuan et al. 2011; Silva Junior et al. 2014; Filipe et al. 2014; Stathi et al. 2006). Metal nanoparticles (NPs) and their combinations have been used for detection of thiocarbamate fungicides such as Thiram and Paraquat (Yuan et al. 2011; Silva Junior et al. 2014; Filipe et al. 2014; Stathi et al. 2006). In this regard, no such reports

Editorial responsibility: M. Borghei.

**Electronic supplementary material** The online version of this article (<https://doi.org/10.1007/s13762-019-02454-9>) contains supplementary material, which is available to authorized users.

✉ B. Mathew  
beenamscs@gmail.com

<sup>1</sup> School of Chemical Sciences, Mahatma Gandhi University, Kottayam, Kerala 686560, India



are available on sensing any dithiocarbamate fungicide utilizing plant extract-capped “green” silver NPs. Here, green-synthesized silver NPs were employed for the detection of Thiram, via UV–Vis spectroscopy, as well as cyclic and differential pulse voltammetric techniques.

As a part of the global efforts to reduce the generation of hazardous waste, “green” methods for synthesis of NPs employing eco-friendly solvents and non-toxic chemicals with ease and least cost are demanded. Green synthesis of noble metal NPs employing phytochemicals has been receiving immense attention since they are eco-friendly and their chemical and physical properties are much dependent on their size and shape. These interesting properties of NPs have found applications in diverse fields, for example, anti-bacterial (Sotiriou and Pratsinis 2010; Tran et al. 2013; Shukla 2014), anti-inflammatory (David et al. 2014; Singh et al. 2017; Moldovan et al. 2017), anticancer (Kajani et al. 2014; Aryal and Bisht 2017; Ovais et al. 2017), catalytic (Crooks et al. 2001; Zhang et al. 2017a, b) and sensing activity (Kubackova et al. 2014; Aravind et al. 2018a, b; Sebastian et al. 2019; Makwana et al. 2017) as well as data storage (Wan et al. 2009; Zheng et al. 2017). In the group, silver NPs occupy a unique status owing to their excellent optical as well as electronic properties. Furthermore, AgNPs are widely used in biological (Vijayan et al. 2017a; Koduru et al. 2018; Da Silva Ferreira et al. 2017; Park et al. 2011; Manikandan et al. 2017; Karthik et al. 2018; Jeyaraj et al. 2013) and environmental applications (Priyadarshini and Pradhan 2017; Joseph and Mathew 2015a; Veisi et al. 2018; Anand et al. 2017; Wu et al. 2017; Potara et al. 2011; Raja et al. 2017; Sebastian et al. 2018) owing to the low toxicity, high stability, cost-effectiveness and ease in handling. Recently, several researchers focused on synthesis of NPs via physical and chemical methods which possess various shortcomings such as multiple steps, high energy requirement, low material conversion, complex purification, and occurrence of hazardous chemicals on the surface. (Joseph and Mathew 2015b; Rafique et al. 2016; Ocoy et al. 2018; Ahmed et al. 2016). Thus, the “greener” methods deserve a great deal of significance in these regards.

Here, *Coscinium fenestratum* (*C.f.*) plant material was employed concurrently as the reducing as well as the capping agent to synthesize and stabilize silver NPs. *C.f.* contains several alkaloids, for example, isoquinoline derivatives such as berberine, palmartine, tetrahydropalmartine, crebaine, and jatrorrhizine (Tushar et al. 2008; Deevanhxay et al. 2009; Akowuah et al. 2014). Hence, *C.f.* has found to receive much attention from researchers for their desired applications. For example, Jacob and co-workers synthesized silver nanorods from the extract of leaves and tender stems of *C.f.* and  $\text{AgNO}_3$  by stirring overnight at room temperature, which showed good cytotoxic activity toward Hep-2 cells (Jacob et al. 2012). The synthetic method used required

many hours, and they employed the nanoparticles only for the cytotoxic study.

The present work demonstrates a simple, one-pot, rapid, microwave production of silver NPs from mature stem extract of the plant *C.f.* and aqueous  $\text{AgNO}_3$  providing the desired particles ( $\text{AgNP-C.f.}$ ) within a few minutes, following principles of green chemistry. Microwave-assisted synthesis of NPs becomes quite a significant method since it provides NPs with size uniformity and faster reaction (Kahrilas et al. 2013; Gawande et al. 2014; Soliveri et al. 2016). Furthermore, owing to the speed of reaction, the agglomeration of NPs can be reduced. In addition, it offers better efficiency, high crystallinity, and better control over the morphology of NPs formed. Consequently, green and microwave-mediated preparation is a promising method for NPs. Advantages of the present work are finer synthesis of silver NPs from the plant *C.f.* and their exploitation for the rapid pollutant organic dye degradation and novel dual sensing of fungicide.

The specific objectives of the current study were to: (1) optimize synthesis conditions like reaction time, ratios of  $\text{AgNO}_3$  and plant extract and power of microwave irradiation; (2) characterize via spectroscopic and microscopic methods such as UV–Vis, FT-IR, X-Ray diffraction (XRD) spectroscopy and transmission electron microscopy (TEM); (3) evaluate sensing of dithiocarbamate fungicide Thiram spectrophotometrically and electrochemically; (4) establish applicability of sensor in real water sample analysis; (5) utilize catalytic activity for the degradation of water pollutant organic dyes like methylene blue, methyl orange, and naphthol green B. The whole study has been conducted in the months of March–May in 2018 at Kottayam, Kerala, India.

## Materials and methods

### Materials

Silver nitrate ( $\text{AgNO}_3$ ), methylene blue, methyl orange, and naphthol green B of analytical grade purity were acquired from Merck (India). Thiram (*N,N*-dimethylcarbamodithioate), from Sigma-Aldrich, was used as such without additional purification. The mature stem of *C.f.*, around 1 cm diameter, was collected in March 2018, from an agricultural nursery, Ernakulam, Kerala, India. 50 g of *C.f.* stem was sliced, washed with water, dried, and stored at room temperature for extract preparation.

### Preparation of *Coscinium fenestratum* stem extract (*C.f.*)

10 g of the *C.f.* stem was boiled in 100 mL of distilled water in a round-bottomed flask fitted with a condenser and water

circulator using a heating mantle. A color change of the solution was observed from colorless to dark yellow indicating the dissolution of compounds in the plant stem into water. After boiling 3 h, the solution was kept to cool to room temperature. Then, the solution was filtered using Whatman No. 1 filter paper, stoppered and stored at 4 °C for synthesis.

### Synthesis of silver nanoparticles using the plant extract

Domestic microwave oven (Sharp R-219T (W)) at an operating power of 200–800 W was used for microwave assistance. 16.9 mg of silver nitrate was dissolved in 100 mL water to acquire a concentration of 1 mM. Further, 90 mL of 1 mM solution was mixed well with 10 mL of the plant extract in a beaker. The resultant solution was microwave irradiated for 9 min, and the reaction was supervised through UV–Vis spectroscopy. 3 mL of the reaction mixture after each 1 min microwave irradiation was taken out using micropipette and irradiated by UV–Vis radiation, and the resultant change in absorbance of the mixture is noted to follow the reaction progress. The formation of a strong peak at about 410 nm showed the production of silver nanoparticles from plant extract.

### Characterization of *Coscinium fenestratum* silver nanoparticles

UV–Vis absorption studies were conducted on Shimadzu UV-2450 spectrophotometer, in the wavelength 200–800 nm. Absorption spectrum of the silver nanoparticle was acquired from 3 mL of its dilute aqueous solution taken in a quartz cuvette. PerkinElmer FT-IR with a frequency range of 400–4000  $\text{cm}^{-1}$  was utilized for functional group analysis of silver nanoparticles. X-ray diffraction studies of the synthesized AgNPs were conducted on a PANalytical X'PERT-PRO X-ray spectrometer with a scan rate of 1.2° per minute and  $2\theta$  is measured from 35° to 80°. The radiation used is Cu  $K\alpha$  (1.5418 Å) with a Ni filter. High-resolution TEM images were gained from a JEOL JEM-2100 microscope. Drop-casting method was used to prepare TEM samples from the silver nanoparticles. An aqueous solution of silver nanoparticles was concentrated by centrifugation. The nanoparticles dispersed in water were then dropped onto carbon-coated copper TEM grids, dried, analyzed, and obtained TEM images in different resolutions.

### Fungicide sensor study

The UV–Vis spectroscopic determination of *N,N*-dimethylcarbamodithioate (Thiram) was carried out in Shimadzu UV-2450 spectrophotometer working from 200 to 800 nm. The sensor studies were carried out with solution of AgNP-*C.f.*

and Thiram at room temperature. The absorption spectrum of AgNP-*C.f.* was followed upon addition of a fixed amount of various concentrations (10–90  $\mu\text{M}$ ) of Thiram. Electrochemical sensing of Thiram was performed on Biologic SP-200 model electrochemical workstation. A platinum electrode was used as the working electrode. Prior to coating with AgNP-*C.f.*, the platinum electrode was cleaned thoroughly with water and later 0.05  $\mu\text{M}$  alumina was used to polish the working surface followed by 1  $\mu\text{M}$  polishing diamond. Subsequently, AgNP-*C.f.* solution was drop cast onto the electrode surface and dried slowly at room temperature. The cyclic voltammogram of the AgNP-*C.f.*-coated platinum electrode was obtained in pH 7 phosphate buffer solution (PBS) in the range of –200 to +1000 mV potential at 100  $\text{mV s}^{-1}$  scan rate. Under similar settings, an interaction between Thiram and AgNP-*C.f.* was observed by addition of Thiram solution to the electrolyte PBS. Selectivity studies were carried out using 100 times higher concentrations of potassium salts of the anions  $\text{CO}_3^{2-}$ ,  $\text{HCO}_3^-$ ,  $\text{Cl}^-$ , carbonates of cations  $\text{Na}^+$ ,  $\text{K}^+$ ,  $\text{Ca}^{2+}$ , and 4-chlorophenol than Thiram addition in UV–Vis as well as voltammetric studies.

Real water sample analysis of Thiram detection was carried out employing differential pulse voltammetric analysis following similar electrochemical system as in cyclic voltammetric studies. Three samples were collected and analyzed to observe the existence of Thiram. Tap water from Mahatma Gandhi University, Kottayam, Kerala, local irrigation canal water from Kottayam, Kerala, and river water from Meenachil River, Kottayam, Kerala, were taken as the samples. Solid particulates were removed from the samples using filtration, and Thiram solution was spiked to the samples for analysis.

### Degradation of water pollutant organic dyes

The common water pollutant dyes, methylene blue ( $8 \times 10^{-5}$  M), methyl orange ( $1 \times 10^{-4}$  M), and naphthol green B ( $1 \times 10^{-4}$  M), were used as sample dyes to study the efficacy of AgNP-*C.f.* for catalytic degradation (Joseph and Mathew 2015a). UV–Vis spectrophotometer was employed to follow the reaction by monitoring the absorbance of the dye. 0.5 mL of freshly prepared  $\text{NaBH}_4$  (0.06 M) solution was added to 2 mL solution of dye in a quartz cuvette. Later, 0.5 mL of AgNP-*C.f.* solution was added to the mixture in the cuvette. At different intervals of time, the UV–Vis spectra were observed at 25 °C.



## Results and discussion

### Synthesis and UV–Vis spectral analysis of *Coscinium fenestratum*-capped silver nanoparticles

1 mM aqueous solutions of silver nitrate and plant extract were mixed, and microwave irradiated by monitoring the reaction using UV–Vis spectroscopy. The progress in the development of NPs was clearly evident from the naked eye visualization of the color of the reaction mixture which intensified and varied from light yellow to yellowish brown. Furthermore, the absorption spectrum also strongly supported the formation of AgNP-*C.f.* by displaying an augment in the absorption band intensity at 423 nm, which symbolizes the surface plasmon resonance (SPR) band, a well-known characteristic of silver nanoparticles (Fig. 1a) (Sharma et al. 2009; Bastús et al. 2015; Shrivastava et al. 2016).

As mentioned earlier, various organic components of the plant extract, such as alcohols, phenols, and aldehydes, reduce  $\text{Ag}^+$  to  $\text{Ag}^0$  and thereby get oxidized by themselves (Ojha et al. 2017; Atarod et al. 2016; Demirbas et al. 2016). The reduction was followed by the conversion of size to the nanoscale. Moreover, the resultant AgNP-*C.f.* was stabilized and thus protected from further agglomeration by the act of the organic compounds, which are constituents of plant extract, since they can concurrently act as capping agents (Saratale et al. 2017; Mallikarjuna et al. 2014; Ahmad et al. 2015; Mahakham et al. 2017). Thus, the “green” approach of metal nanoparticle synthesis involving plant extracts replaces the perilous chemicals used as reducing as well as capping agents by the safe and cheaper organic compounds.

Furthermore, the synthesis of AgNP-*C.f.* from the plant extract was optimized by controlling factors such as ratios of silver nitrate solution and plant extract, the power of microwave irradiation, and time of irradiation. The reaction was carried out in three different ratios of 1 mM aqueous silver nitrate and plant extract such as 9:1, 4:1, and 2:1 where the power of irradiation and time were kept constant. From absorption spectra, it was revealed that the formation of AgNP-*C.f.* was efficient when the ratio was 9:1. Similarly, the power of microwave irradiation was varied as 200, 400, 600, and 800 W, where the ratio of silver nitrate and plant extract and time were kept constant and observed 600 W as the power resulting in efficient synthesis. Moreover, the optimum time of microwave irradiation to obtain the better synthesis of nanoparticle was optimized as 9 min, while ratio and power were constant. From these results, one can conclude that the formation of AgNP-*C.f.* was efficient when 1 mM aqueous solutions of silver nitrate and plant extract when mixed in 9:1 ratio was irradiated with a microwave of power 600 W for 9 min. The absorption spectra illustrating the optimization are provided in Figure S1 (Supporting Material (SM)). AgNP-*C.f.* was found to be very stable for 6 months when stored at 4 °C as shown by the absorption spectrum which displayed no observable changes in comparison with the freshly prepared AgNP-*C.f.* This indicates the lesser tendency of agglomeration in the nanoparticle solution and thus the efficiency of phytochemicals in the role of a capping agent.

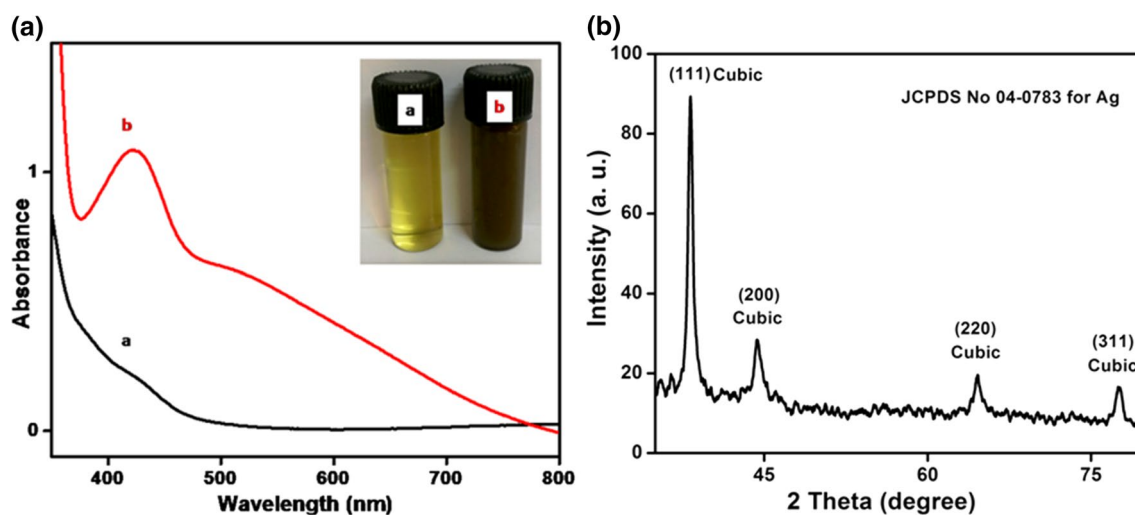


**Fig. 1** (a) UV–Vis absorption spectra and photograph (inset) of (a) *C.f.* extract, and (b) AgNP-*C.f.*; (b) XRD pattern of AgNP-*C.f.*

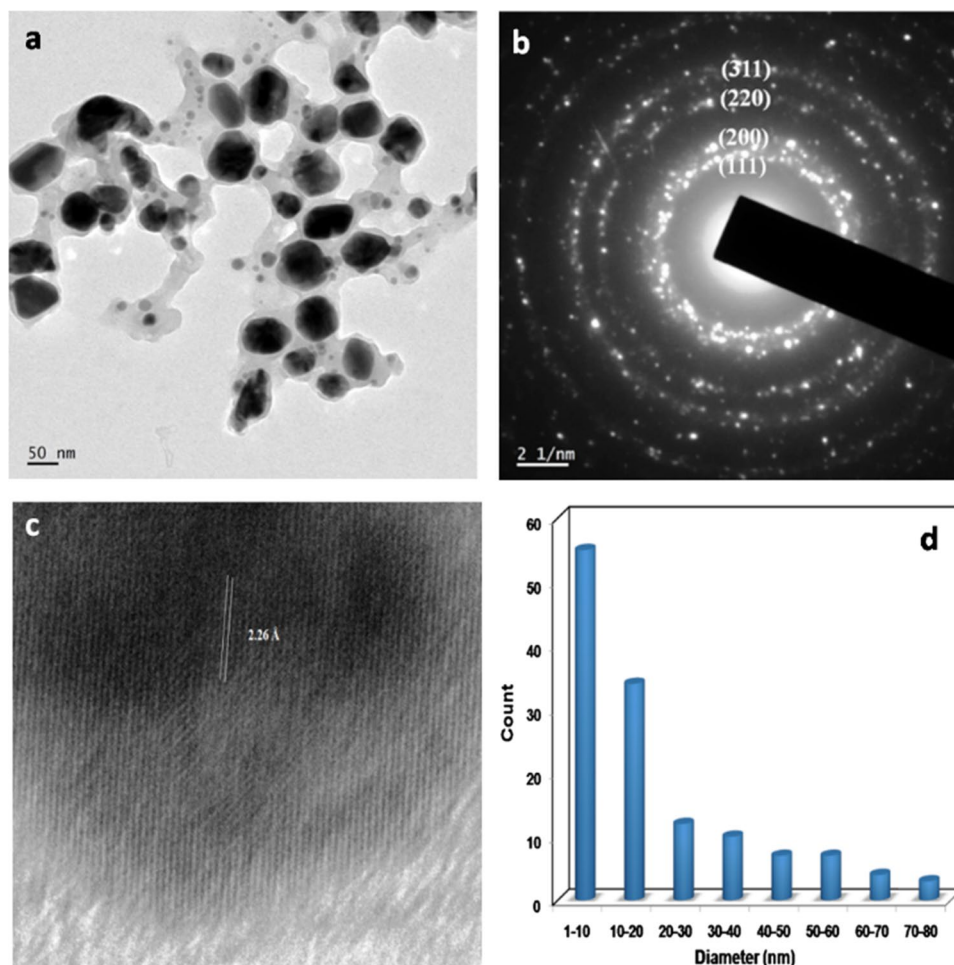
## Fourier transform-infrared (FT-IR) spectroscopic study

The FT-IR spectrum provides information regarding the functional groups present in the plant extract such as hydroxyl groups, which are capable of reducing the  $\text{Ag}^+$  to AgNPs. The FT-IR spectrum revealed the presence of alcohol, ether functionalities, aromatic rings, and amines. For example, broad peak at  $3340\text{ cm}^{-1}$  indicates the occurrence of  $-\text{OH}$ ,  $-\text{NH}_2$ , and aliphatic  $-\text{CH}$  stretching vibrations, which gave strong evidence for the presence of amines and alcohols in the plant extract, acts as capping agent during the formation of AgNP-*C.f.* Furthermore, as discussed earlier, aromatic components like berberine and palmatine (chief alkaloids) were present in plant extract and hence furnished aromatic C–H stretching vibration and  $-\text{C}=\text{C}$  stretching peak at  $2940$  and  $1505\text{ cm}^{-1}$ , respectively. Moreover, the band at  $1602$  and  $1326\text{ cm}^{-1}$  attributes to  $-\text{N}-\text{H}$  bending and  $-\text{C}-\text{N}$  stretching, respectively, giving a strong indication of amines in the plant extract. The presence of aromatic ethers showed bands at  $1074$  and  $1026\text{ cm}^{-1}$  for  $-\text{C}-\text{O}$  stretch of  $-\text{OCH}_3$  (Fig. 6a).

## X-ray diffraction (XRD) study

The XRD studies endow with information concerning the chemical identity and crystallinity of the substance. The prepared AgNP-*C.f.* exhibited four peaks in the XRD spectrum, one intense and three less intense. As shown in Fig. 1b, the XRD pattern shows diffraction peaks at  $2\theta$  values  $38.22^\circ$ ,  $44.41^\circ$ ,  $64.62^\circ$ , and  $77.56^\circ$ . In comparison with the JCPDS file number 04-0783, peaks obtained at the given  $2\theta$  values can be assigned to cubic phase, with the reflections from the planes (111), (200), (220), and (311) of the face-centered cubic lattice of silver nanoparticles (Joseph and Mathew 2015a). Scherrer equation endow with the crystallite size (average) of the particles as  $16.34\text{ nm}$ . The lattice parameter obtained from XRD data was  $4.07\text{ nm}$ , which is in fine union with the JCPDS file of silver nanoparticles ( $4.08\text{ nm}$ ). Furthermore, the X-ray diffraction pattern of the synthesized AgNP-*C.f.* establishes undoubtedly the crystallinity of silver nanoparticles.

**Fig. 2** TEM images of AgNP-*C.f.* **a** at inset bar  $50\text{ nm}$ ; **b** SAED pattern showing the different planes present; **c** HR-TEM image, and **d** particle size distribution histogram



## Transmission electron microscopy (TEM) analysis

TEM images of nanoparticles deliver significant features about the average size, shape, along with morphology through a clear image of the particle surface. The surface morphology analysis of AgNP-*C.f.* using TEM images shows the almost spherical shape as evident from Fig. 2a.

Moreover, the TEM image (Fig. 2a) clearly evidences the existence of the organic layer present around the nanoparticles supporting their role as the capping agent. The selected area electron diffraction (SAED) pattern of the nanoparticles, displayed in Fig. 2b, has circular rings indicating the face-centered cubic lattice of silver nanoparticles. The rings from inside to outside represent the reflections from the planes (111), (200), (220), and (311), respectively (Joseph and Mathew 2015a). Lattice fringes visualized in the HR-TEM image (Fig. 2c) evidences the crystallinity of obtained nanoparticles and d-spacing between particle layers in the planes. Furthermore, the d-spacing was found as 2.26 Å, suggesting that the nanoparticle growth occur predominantly on the (111) plane. Size allocation of AgNP-*C.f.* is obtained by analyzing the TEM images and is represented in the histogram (Fig. 2d). The particles are less monodisperse similar to many of the phytochemical-stabilized silver nanoparticles. Size of AgNP-*C.f.* was found in the region of 10–30 nm, and average diameter was  $20.72 \pm 4.25$  nm.

## Fungicide sensing study

Thiram is a non-systemic fungicide, also used as ectoparasiticide and as an animal repellent to control animal attack to crops. It is commonly used in agriculture of apple, strawberry, pears, soybean, wine yards, peaches, and tea in many parts of the world and in India. However, its extensive use

has lead to contamination of environmental water and thus marked as a noted pollutant (Yuan et al. 2011). Exposure to Thiram causes skin, eye irritation, and damage of the liver as a result of the release of carbon disulfide and hence Thiram detection is significant (Sharma et al. 2003). Accordingly, the phytochemical-based AgNP-*C.f.* was studied as the eco-friendly sensor for monitoring the presence of Thiram (Figure S3 in SM) in environment employing UV–Vis spectroscopy, cyclic voltammetry along with differential pulse voltammetry.

In UV–Vis spectroscopy, the change in absorbance value of SPR peak of AgNP-*C.f.* at 423 nm was followed upon addition of 10–90 μM concentrations of Thiram. The absorption band of AgNP-*C.f.* was decreased upon sequential addition of fixed amounts of Thiram which can be credited to the intermolecular H-bonding interactions among Thiram and the functional groups present in the capping organic molecules. Furthermore, the selectivity studies of AgNP-*C.f.* toward Thiram were conducted among various competent species possible to present in water samples such as Na<sup>+</sup>, K<sup>+</sup>, Ca<sup>2+</sup>, CO<sub>3</sub><sup>2-</sup>, HCO<sub>3</sub><sup>-</sup>, Cl<sup>-</sup>, and 4-chlorophenol. There is a very feeble change in the absorption band of AgNP-*C.f.* upon addition of Na<sup>+</sup>, K<sup>+</sup>, Ca<sup>2+</sup>, CO<sub>3</sub><sup>2-</sup>, HCO<sub>3</sub><sup>-</sup>, Cl<sup>-</sup>, and 4-chlorophenol, whereas upon addition of Thiram, there observed reasonable changes, which indicate that the AgNP-*C.f.* is selective toward Thiram (Fig. 3).

Furthermore, the electrochemical sensing ability of AgNP-*C.f.* was investigated toward Thiram (Fig. 4). AgNP-*C.f.*-coated platinum electrode was the working electrode, while Ag/AgCl electrode and platinum wire were used as the reference electrodes. The sensing ability of AgNP-*C.f.* toward Thiram was studied by adding fixed quantities of 10–90 μM Thiram solutions in phosphate buffer solutions (PBS) as the electrolyte. Furthermore, the pH of the buffer

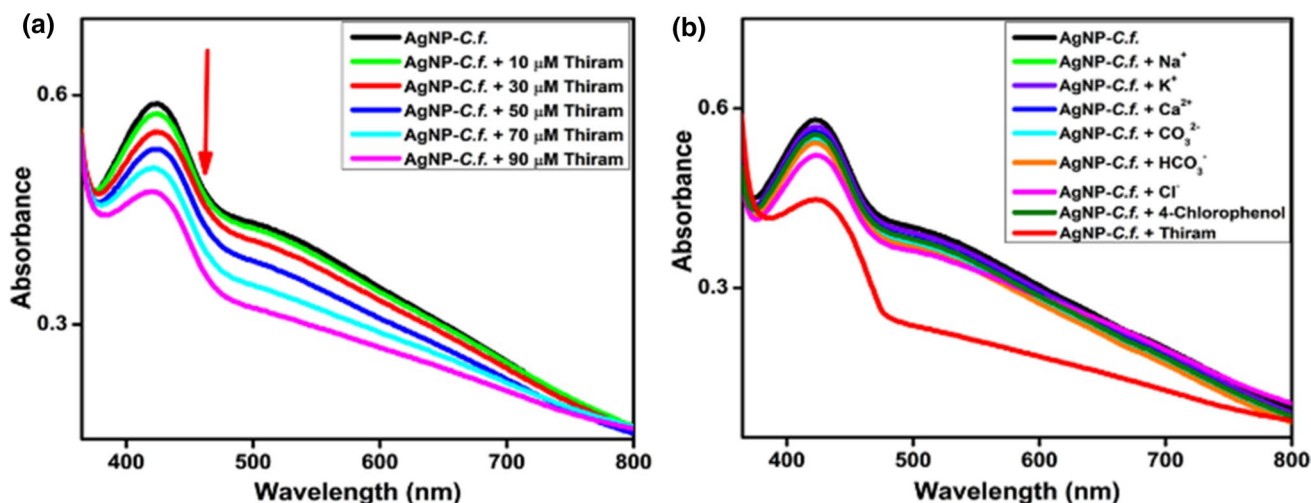
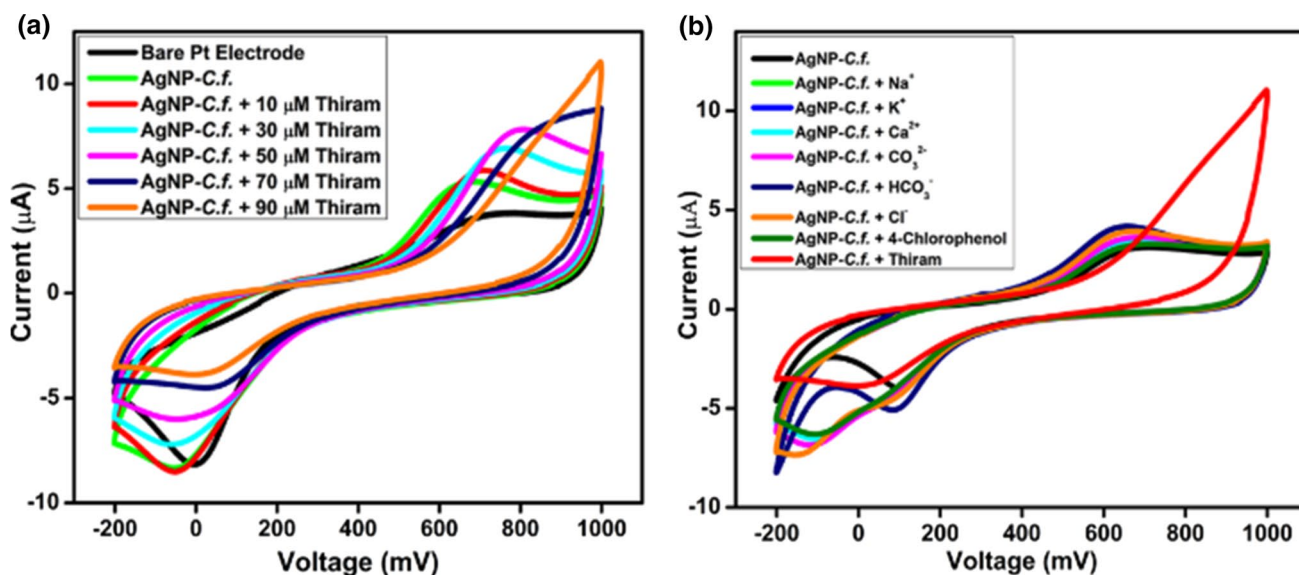


Fig. 3 UV–Vis spectra of AgNP-*C.f.* upon addition of a 10–90 μM Thiram, and b fixed amounts of competitive species and Thiram



**Fig. 4** Cyclic voltammogram of AgNP-C.f. after addition of **a** 10–90  $\mu\text{M}$  Thiram **b** fixed amounts of competitive species and Thiram

solution and scan rate of voltammetric experiments was optimized to 7 and 100  $\text{mV s}^{-1}$ , respectively (Figure S4 in SM). The area of voltammogram increased remarkably upon coating of AgNP-C.f. onto the active surface of the platinum electrode when compared to the bare electrode. Addition of 10–90  $\mu\text{M}$  Thiram solutions to the electrolyte leads to a sequential increase in the oxidation peak of the voltammogram. The shape of voltammogram changed with the enhancement in the concentration of Thiram solution. Moreover, with the intention to find out the selectivity toward a particular analyte, the selectivity study of AgNP-C.f. was carried out upon addition of various species such as  $\text{Na}^+$ ,  $\text{K}^+$ ,  $\text{Ca}^{2+}$ ,  $\text{CO}_3^{2-}$ ,  $\text{HCO}_3^-$ ,  $\text{Cl}^-$ , and 4-chlorophenol. There is a null or little change in the voltammogram of AgNP-C.f. in the presence of these species when compared to the addition of Thiram which showed notable changes. From these results, one can conclude that AgNP-C.f. was selective toward Thiram.

To acquire the limit of detection of Thiram by AgNP-C.f., the differential pulse voltammetric (DPV) technique was utilized. DPV was conducted in the same electrode system, and electrolytes were used as same as cyclic voltammetry. The DPV experiment was performed for AgNP-C.f. upon addition of fixed amounts of 10–90  $\mu\text{M}$  concentrations of Thiram solutions to the electrolyte buffer solution. The linear increment in current was observed upon addition of 10–90  $\mu\text{M}$  concentrations of Thiram solutions. Figure 5 shows the differential pulse voltammogram of AgNP-C.f. with various concentrations of Thiram.

From the current obtained at fixed potential subsequent to the addition of each concentration of the fungicide, a correlation graph of concentration of fungicide versus the

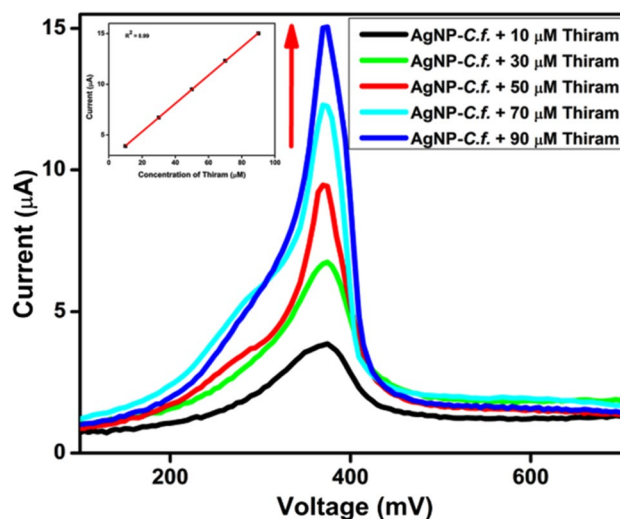


**Fig. 5** Differential pulse voltammogram of AgNP-C.f. in the presence of 10–90  $\mu\text{M}$  of Thiram; inset shows the correlation graph of concentration of Thiram versus current

obtained current was plotted. We gained a linear plot with a regression coefficient of 0.99. Analysis of data provided the limit of detection as 0.731  $\mu\text{M}$  or 0.18 ppm which was much lesser than the maximal residue limit (MRL) of Thiram, 7 ppm allowed in fruit peels, as per the Environmental Protection Agency of United States (EPA) (Yuan et al. 2011). The limit of detection obtained has been compared with the literature reports and found that AgNP-C.f. is efficient than many materials employing toxic chemicals (Table 1).

Accordingly, the green-synthesized nanoparticles AgNP-C.f. can be employed as an efficient sensor for monitoring

**Table 1** Comparison of Thiram detection by AgNP-C.f. with reports

Methods	Limit of detection	References
CN-DTC-Ag NPs	$2.8 \times 10^{-6}$ M	Rohit and Kailasa (2014)
C <sub>18</sub> -SPE	$1.4 \times 10^{-6}$ M	Filipe et al. (2007)
Sodium molybdate	$1.3 \times 10^{-6}$ M	Sharma et al. (2005)
Iron(II) and Cobalt(II) phthalocyanines	$40.0 \times 10^{-6}$ M	Shaidarova et al. (2001)
AgNP-C.f.	$0.7 \times 10^{-6}$ M	This work

the thiocarbamate fungicide, Thiram, and it might be useful in monitoring the fungicide in fruit peels as well as real sample analysis.

### FT-IR and TEM analysis of Thiram-treated *Coscinium fenestratum* silver nanoparticles

To better understand the interaction between the fungicide and AgNP-C.f., FT-IR and TEM analyses of AgNP-C.f. in the presence of Thiram were performed (Fig. 6).

Comparison of FT-IR spectra of AgNP-C.f. in the presence and absence of Thiram revealed that the intensity of the vibration bands decreased in the presence of fungicide. The intensity of bands centered at 3340, 1602, 1326, and 1026  $\text{cm}^{-1}$  was observed to decrease particularly indicating the involvement of the corresponding functional groups such as  $-\text{OH}$ ,  $-\text{NH}_2$ , and  $-\text{OCH}_3$ , in interaction with Thiram generating changes in UV-Vis and cyclic voltammetric spectra. Additional few sharp weak bands appeared in the spectra of AgNP-C.f. in presence of Thiram which might be due to the additional bond vibrations from the fungicide. The evaluation of TEM images of AgNP-C.f. with and without the addition of Thiram shows clear aggregation of the nanoparticles upon addition of Thiram and hence the uneven distribution of the particles (Rohit and Kailasa 2014). These evidences

clarify the interaction of the silver nanoparticles with the fungicide moiety. Moreover, the selected area electron diffraction (SAED) image of AgNP-C.f. and AgNP-C.f.-Thiram was compared and one can observe that the latter have much fader spots when compared to the former. It indicates the decrease in crystallinity of the silver nanoparticles after interaction with Thiram.

Furthermore, the relevance of the sensor in real water sample analysis was tested using differential pulse voltammetric analysis in tap, canal, and river water samples. The sensor could detect 99% of Thiram from the water samples indicating its efficiency in real-time monitoring. The results are displayed in Table 2.

### Degradation of water pollutant organic dyes

The water resources have been vastly polluted by the dumping of colored organic dye wastes from various industries like textile, printing, food, paint, and lot more (Singh et al. 2015; Ghaly et al. 2014; Jin et al. 2006). Water polluted by organic dyes is reported to create several health issues to terrestrial and aquatic life (Davydov et al. 2001; Mathur et al. 2006; Rajaguru et al. 2003). Hence, researchers have invested a good deal of effort toward destruction of such toxic organic dyes by obtaining materials which are cheap and easy to prepare as well as fast and efficient in action. Methyl orange or sodium; 4-[[4-(dimethylamino)phenyl]diazanyl]benzenesulfonate is an organic azo dye

**Table 2** Real water sample analysis of Thiram by AgNP-C.f

Samples	Thiram ( $\mu\text{M}$ )		Detected (%)
	Added	Found	
Tap water	10	$10.03 \pm 0.004$	$99.7 \pm 0.003$
Local canal water	10	$10.04 \pm 0.003$	$99.6 \pm 0.002$
Meenachil river water	10	$10.08 \pm 0.004$	$99.2 \pm 0.003$

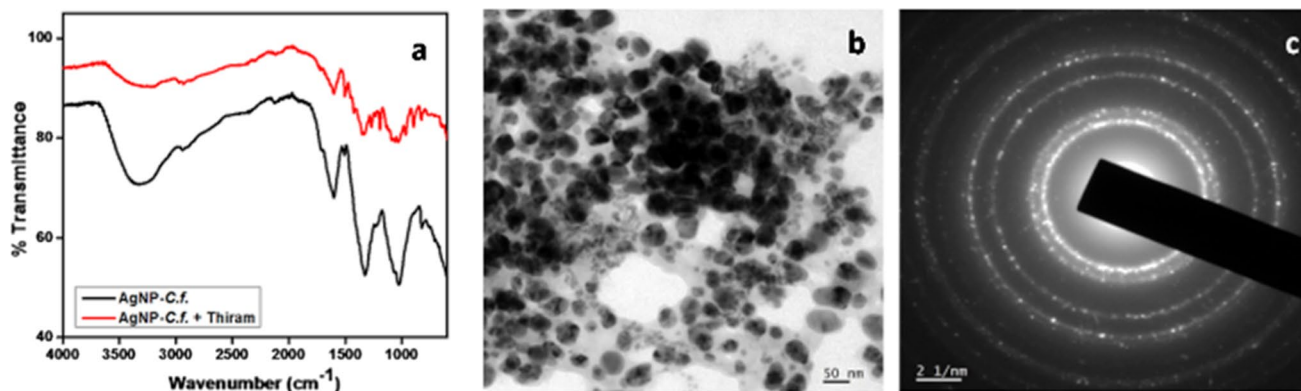


**Fig. 6** a FT-IR spectra of AgNP-C.f. in the presence and absence of Thiram; b TEM image, and c SAED pattern of AgNP-C.f. in the presence of Thiram



giving orange-red color in aqueous solution and used as an indicator for various analytical fields (Mittal et al. 2007). Naphthol green B or trisodium;iron(3<sup>+</sup>);5-nitroso-6-oxidonaphthalene-2-sulfonate is an acidic nitroso dye which has a strong affinity for proteins and used in dyeing of anodized aluminum, coating and surface coloring of paper, cosmetics, and drugs for external use (Gurr 1971). Methylene blue, also known as methylthioninium chloride, is a basic aniline dye useful in the diverse field of research such as basic science, medicine and so forth. Methylene blue is well known as an indicator of redox reactions as well as a stain that assists in the identification of bacteria in biology. In the medical field, it is used for the treatment of methemoglobinemia, and manic-depressive psychosis, and as a urinary antiseptic, analgesic, antipyretic, antiparasitic, and antimalarial (Clifton and Leikin 2003; Rafatullah et al. 2010).

Nanomaterials hold a majority of recent advances in the discovery of efficient materials for remediation of water polluted by organic dyes (Perreault et al. 2015; Kumar et al. 2014; Tan et al. 2015; Santhosh et al. 2016). Among them, silver nanoparticles synthesized from plants are predominantly valuable since they are synthesized obeying principles of green chemistry, and are least toxic, easy to prepare, fast and efficient catalysts in dye degradation (Bhakya et al. 2015; Vijayaraghavan and Ashokkumar 2017; Bogireddy et al. 2016). Recently, our research group has published works on the production of silver and gold nanoparticles via phytochemical methods and the degradation of organic dyes (Vijayan et al. 2017b; Francis et al. 2017; Joseph and Mathew 2015c). Encouraged by these results, AgNP-C.f. was employed for the destruction of pollutant organic dyes such as methyl orange, methylene blue, and naphthol green B with NaBH<sub>4</sub> as the reducing agent (Figure S5 in SM). Notably, dye degradation studies showed that AgNP-C.f. catalyzes complete degradation of dyes much faster when compared to the previous results (Vijayan et al. 2017b; Francis et al. 2017; Joseph and Mathew 2015c).

The degradation of dyes was studied with and without the addition of the nanocatalyst, AgNP-C.f. The dyes were treated with NaBH<sub>4</sub> alone and observed no change in color as well as the absorbance of the three dyes even after 4 h. From these results, one can conclude that the degradation using only NaBH<sub>4</sub> is negligibly slow. Thus, AgNP-C.f. was employed as nanocatalyst along with NaBH<sub>4</sub>, to improve the degradation rate of above-mentioned dyes. The absorption bands of methyl orange, naphthol green B, and methylene blue was found to be at 464, 715, and 663 nm, respectively, in aqueous solutions. The degradation studies of these organic dyes were monitored by means of UV–Vis spectroscopy. The absorption of dyes was fully diminished, and the color of the solution bleached off completely upon addition of nanocatalyst (AgNP-C.f.) along with NaBH<sub>4</sub>.

These studies were carried out in detail with different concentration of AgNP-C.f. For example, 0.01 mg/mL of AgNP-C.f. leads to complete degradation of methyl orange in 9 min, whereas for the others, naphthol green B and methylene blue, the absorption peak was completely diminished with 12 and 4 min, respectively (Figure S6 in SM). Furthermore, control studies were performed for these dyes in the absence of AgNP-C.f. and found no change or a slight change in absorption spectra even after few hours. These results revealed that AgNP-C.f. acts as proficient nanocatalyst for degradation of pollutant dyes in the presence of NaBH<sub>4</sub>. Additionally, the degradation study of the three dyes was performed in higher concentrations of AgNP-C.f. such as 0.03 (Figure S7 in SM) and 0.05 mg/mL (Fig. 7), while the quantity and concentration of the dye, as well as NaBH<sub>4</sub>, were kept unchanged. The concentration 0.03 mg/ml of AgNP-C.f. effected complete degradation of methyl orange, naphthol green B, and methylene blue within 4, 7, and 2 min, respectively, while a higher concentration of 0.05 mg/mL AgNP-C.f., degraded the first two dyes in 3 and 4 min, respectively, and methylene blue instantaneously.

These results definitely stand out from similar reports by a significant decrease in reaction time and thus the AgNP-C.f.

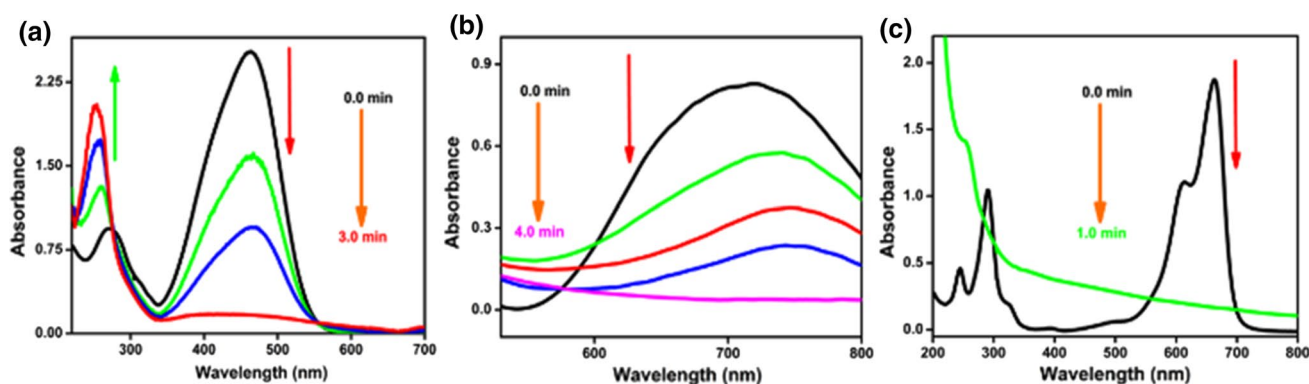


**Fig. 7** Degradation study of **a** methyl orange, **b** naphthol green B, and **c** methylene blue with NaBH<sub>4</sub> in the presence 0.05 mg/mL AgNP-C.f



catalyst is very promising for real-time water treatment applications. In the process of degradation, bubbles were produced on the surface of the AgNP-*C.f.* catalyst, indicating the formation of hydrogen gas. The hydrogen gas generated plays a key role in the removal of oxygen from the reaction which avoids the re-oxidation of leuco methylene blue into colored methylene blue. Hydrogen gas also aids to remove the products obtained from the surface of catalyst keeping the surface fresh (Joseph and Mathew 2015a), which might increase the efficiency of the catalyst.

For evaluation of the rate of catalytic degradations, the degradation kinetics of the three water pollutant organic dyes were studied by monitoring their absorption peaks. The chemistry behind the dye- $\text{NaBH}_4$  interaction is believed as an electron transfer, where the dyes act as electrophilic and the  $\text{BH}_4^-$  ions act as nucleophilic centers. AgNP-*C.f.* catalyzes this reaction by providing a platform for  $\text{BH}_4^-$  and dye to approach closer and permit the relay of electrons of donor  $\text{BH}_4^-$  to dye which is the acceptor.

The capping agents help to bring the donor and acceptor in close proximity. This offers a substitute pathway of lower energy of activation and makes the degradation kinetically viable (Joseph and Mathew 2015c). In this process, since electron transfer occurs from  $\text{BH}_4^-$  to dyes, the concentration of  $\text{BH}_4^-$  added in the system is much higher in comparison with AgNP-*C.f.* Moreover, the concentration of  $\text{NaBH}_4$  remains constant while that of AgNP-*C.f.* is varied, results in a pseudo-first-order reaction. The pseudo-first-order kinetics is represented as follows:  $\ln[A]/[A_0] = -kt$  where  $[A]$  is the dye concentration at time ' $t$ ' which can be acquired from the absorbance peak of dyes,  $[A_0]$  is the concentration of dyes at time  $t=0$ , and  $k$  is the pseudo-first-order rate constant. Calibration curve of absorbance versus concentration is provided in the supplementary material (Figure S8 in SM). Furthermore, the graph between  $\ln[A]$  against time ( $t$ ) was plotted for the degradation of dyes using the different concentrations of nanocatalyst as shown in Fig. 8.

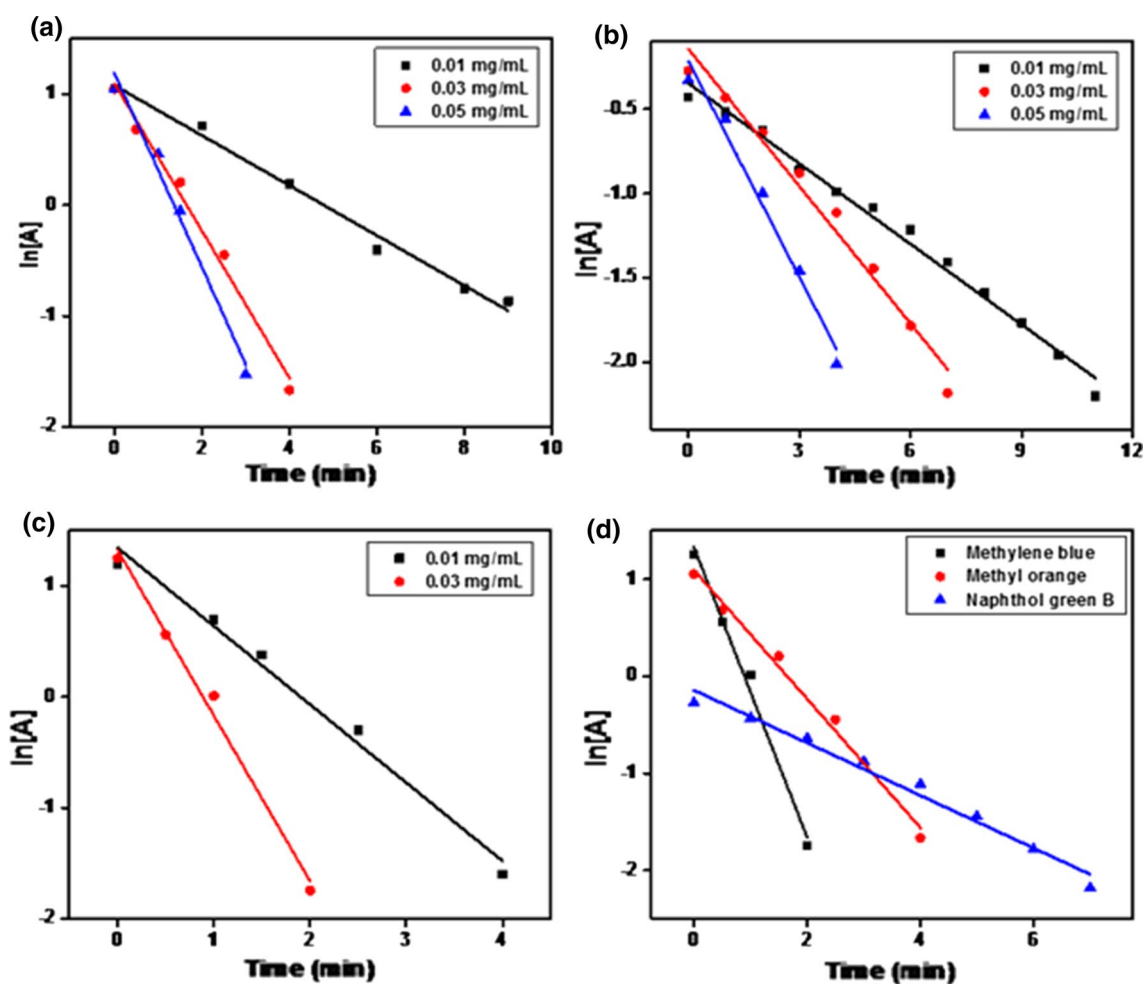


**Fig. 8** Kinetics study of dye degradation with  $\text{NaBH}_4$  in the presence of AgNP-*C.f.* **a** methyl orange, **b** naphthol green B, **c** methylene blue, and **d** comparison of degradation kinetics of three dyes at catalyst concentration = 0.03 mg/ml

The graph was found to be linear for all dyes, which validates the pseudo-first-order kinetics of the degradation reaction. The correlation coefficients obtained were in the region of 0.975–0.989 (Table S1 in SM). A notable increment was observed in the reaction rate with an enhancement in the concentration of AgNP-*C.f.*, which might be due to enhanced availability of catalyst surface area. Furthermore, the rate constant,  $k$ , was gained from the slope of  $\ln[A]$  versus time ( $t$ ) plot as per the rate equation:  $k = 1/t \ln[A_0]/[A]$ . Table S1 in SM presented the relationship between the concentrations of catalyst used, the time taken for degradation and rate constants of the three dyes. Rate constant was highest for MB ( $k = 1.49$ , at 0.03 mg/mL) among the dyes and it was higher for MO ( $k = 0.66$ , at 0.03 mg/mL) than NGB ( $k = 0.27$ , at 0.03 mg/mL). Also, the rate constants increased with an increase in the concentration of AgNP-*C.f.* as expected. The study confirms the utility of AgNP-*C.f.* as an extremely efficient catalyst for organic pollutant degradation which makes them desirable in environmental remediation.

## Conclusion

Green nanoparticles obtained via express, effortless, and economic method were employed for fungicide detection and pollutant degradation as a part of the goal toward environmental remediation. Microwave-assisted production of silver nanoparticles using aqueous silver nitrate and the stem extract of the plant *C. f.* in merely water medium ensured minimum toxicity effects to the environment during the production. The chief alkaloids present in *C. f.* extract like berberine and palmatine act concurrently as the reducing and capping agents in the synthesis, avoiding the use of any toxic chemicals. AgNP-*C.f.* was successfully characterized using UV-Vis, FT-IR, XRD, and TEM analyses. UV-Vis spectroscopic studies primarily evidenced the formation of nanoparticles, while FT-IR demonstrated the existence of organic functional groups in the plant extract. The crystallinity and face-centered cubic lattice of the NPs were proved by XRD, and morphology was obtained by TEM analysis. The nanoparticles were mostly spherical shaped, and average diameter was  $20.72 \pm 4.25$  nm. The nanoparticles were exploited for the detection of a fungicide Thiram, and degradation of common water pollutant organic dyes AgNP-*C.f.* displayed sensitivity and selectivity toward the dithiocarbamate fungicide, Thiram with LOD = 0.18 ppm, much lower than MRL (7 ppm) by the US Agency, EPA and were successfully detecting the fungicide in spiked water samples from tap, canal, and river. Furthermore, the catalytic efficiency was so prominent to bring about the complete degradation of water pollutant acidic dye methylene blue instantaneously while that of methyl orange and naphthol

green B within a couple of minutes. Thus, one can find the green-synthesized AgNP-*C.f.* as a promising candidate for practical applications in detection of Thiram and dye degradation. Even though rapid dual sensing of dithiocarbamate fungicide was achieved in micro-molar levels using AgNP-*C.f.*, the nanoparticles can be further modified with some non-toxic component to achieve nanomolar-level sensing.

**Acknowledgements** Ragam N. Priyanka is grateful to Kerala State Council for Science Technology and Environment (KSCSTE), Kerala, India, for Research Fellowship.

## Compliance with ethical standards

**Conflict of interest** There are no conflicts to declare.

## References

- Ahmad A et al (2015) Silver and gold nanoparticles from *Sargentodoxa acuneata*: synthesis, characterization and antileishmanial activity. *RSC Adv* 5(90):73793–73806. <https://doi.org/10.1039/c5ra13206a>
- Ahmed S et al (2016) A review of plants extract mediated synthesis of silver nanoparticles for antimicrobial applications: a green expertise. *J Adv Res* 7(1):17–28. <https://doi.org/10.1016/j.jare.2015.02.007>
- Akowuah GA, Okechukwu PN, Chiam NC (2014) Evaluation of HPLC and spectrophotometric methods for analysis of bioactive constituent berberine in stem extracts of *Coscinium fenestratum*. *Acta Chromatogr* 26(2):243–254. <https://doi.org/10.1556/achrom.26.2014.2.4>
- Anand K et al (2017) Bio-synthesis of silver nanoparticles using agroforestry residue and their catalytic degradation for sustainable waste management. *J Clust Sci* 28(4):2279–2291. <https://doi.org/10.1007/s10876-017-1212-2>
- Aravind A, Sebastian M, Mathew B (2018a) Green silver nanoparticles as a multifunctional sensor for toxic Cd(II) ions. *New J Chem* 42(18):15022–15031. <https://doi.org/10.1039/c8nj03696a>
- Aravind A, Sebastian M, Mathew B (2018b) Green synthesized unmodified silver nanoparticles as a multi-sensor for Cr(III) ions. *Environ Sci Water Res Technol* 4(10):1531–1542. <https://doi.org/10.1039/c8ew00374b>
- Aryal S, Bisht G (2017) New paradigm for a targeted cancer therapeutic approach: a short review on potential synergy of gold nanoparticles and cold atmospheric plasma. *Biomedicines* 5(4):38. <https://doi.org/10.3390/biomedicines5030038>
- Atarod M, Nasrollahzadeh M, Mohammad Sajadi S (2016) Euphorbia heterophylla leaf extract mediated green synthesis of Ag/TiO<sub>2</sub> nanocomposite and investigation of its excellent catalytic activity for reduction of variety of dyes in water. *J Colloid Interface Sci* 462:272–279. <https://doi.org/10.1016/j.jcis.2015.09.073>
- Bastús NG, Piella J, Puentes V (2015) Quantifying the sensitivity of multipolar (dipolar, quadrupolar, and octapolar) surface plasmon resonances in silver nanoparticles: the effect of size, composition, and surface coating. *Langmuir* 32(1):290–300. <https://doi.org/10.1021/acs.langmuir.5b03859>
- Bhakya S et al (2015) Catalytic degradation of organic dyes using synthesized silver nanoparticles: a green approach. *J Bioremed Biodegrad*. <https://doi.org/10.4172/2155-6199.1000312>
- Bogireddy NKR, Kiran Kumar HA, Mandal BK (2016) Biofabricated silver nanoparticles as green catalyst in the degradation of



- different textile dyes. *J Environ Chem Eng* 4(1):56–64. <https://doi.org/10.1016/j.jece.2015.11.004>
- Cereser C et al (2001) Thiram-induced cytotoxicity is accompanied by a rapid and drastic oxidation of reduced glutathione with consecutive lipid peroxidation and cell death. *Toxicology* 163(2–3):153–162. [https://doi.org/10.1016/s0300-483x\(01\)00401-2](https://doi.org/10.1016/s0300-483x(01)00401-2)
- Clifton J, Leikin JB (2003) Methylene blue. *Am J Ther* 10(4):289–291. <https://doi.org/10.1097/00045391-200307000-00009>
- Crooks RM et al (2001) Dendrimer-encapsulated metal nanoparticles: synthesis, characterization, and applications to catalysis. *Acc Chem Res* 34(3):181–190. <https://doi.org/10.1021/ar000110a>
- Da Silva Ferreira V et al (2017) Green production of microalgae-based silver chloride nanoparticles with antimicrobial activity against pathogenic bacteria. *Enzyme Microb Technol* 97:114–121. <https://doi.org/10.1016/j.enzmictec.2016.10.018>
- David L et al (2014) Green synthesis, characterization and anti-inflammatory activity of silver nanoparticles using European black elderberry fruits extract. *Colloids Surf B* 122:767–777. <https://doi.org/10.1016/j.colsurfb.2014.08.018>
- Davydov L et al (2001) Sonophotocatalytic destruction of organic contaminants in aqueous systems on TiO<sub>2</sub> powders. *Appl Catal B* 32(1–2):95–105. [https://doi.org/10.1016/s0926-3373\(01\)00126-6](https://doi.org/10.1016/s0926-3373(01)00126-6)
- Deevanhay P et al (2009) Simultaneous characterization of quaternary alkaloids, 8-oxoprotoberberine alkaloids, and a steroid compound in *Coscinium fenestratum* by liquid chromatography hybrid ion trap time-of-flight mass spectrometry. *J Pharm Biomed Anal* 50(3):413–425. <https://doi.org/10.1016/j.jpba.2009.05.023>
- Demirbas A, Welt BA, Ochoy I (2016) Biosynthesis of red cabbage extract directed Ag NPs and their effect on the loss of antioxidant activity. *Mater Lett* 179:20–23. <https://doi.org/10.1016/j.matlet.2016.05.056>
- Fei Chan Y et al (2013) Ag dendritic nanostructures as ultrastable substrates for surface-enhanced Raman scattering. *Appl Phys Lett* 102(18):183118. <https://doi.org/10.1063/1.4803937>
- Filipe OMS et al (2007) A solid-phase extraction procedure for the clean-up of thiram from aqueous solutions containing high concentrations of humic substances. *Talanta* 72(3):1235–1238. <https://doi.org/10.1016/j.talanta.2007.01.005>
- Filipe OMS et al (2014) Effect of copper ions on the degradation of thiram in aqueous solution: identification of degradation products by HPLC–MS/MS. *J Hazard Mater* 279:125–132. <https://doi.org/10.1016/j.jhazmat.2014.06.051>
- Francis S et al (2017) Synthesis and characterization of multifunctional gold and silver nanoparticles using leaf extract of *Naregamiaalata* and their applications in the catalysis and control of mastitis. *New J Chem* 41(23):14288–14298. <https://doi.org/10.1039/c7nj02453c>
- Gawande MB et al (2014) Microwave-assisted chemistry: synthetic applications for rapid assembly of nanomaterials and organics. *Acc Chem Res* 47(4):1338–1348. <https://doi.org/10.1021/ar400309b>
- Ghaly AE et al (2014) Production, characterization and treatment of textile effluents: a critical review. *J Chem Eng Process Technol*. <https://doi.org/10.4172/2157-7048.1000182>
- Gurr E (1971) *DISPERSE DYES*. Synthetic dyes in biology, medicine and chemistry. Academic Press, Elsevier, pp 691–702. ISBN 9780123096500. <https://doi.org/10.1016/b978-0-12-309650-0.50013-2>
- Hasan H (2010) Fungicides and their effects on animals. *Fungicides*. <https://doi.org/10.5772/12959>
- Jacob SJP et al (2012) Synthesis of silver nanorods using *Coscinium fenestratum* extracts and its cytotoxic activity against Hep-2 cell line. *Colloids Surf B* 98:7–11. <https://doi.org/10.1016/j.colsurfb.2012.03.031>
- Jeyaraj M et al (2013) Biogenic silver nanoparticles for cancer treatment: an experimental report. *Colloids Surf B* 106:86–92. <https://doi.org/10.1016/j.colsurfb.2013.01.027>
- Jin X-C et al (2006) Decolorization of a dye industry effluent by *Aspergillus fumigatus* XC6. *Appl Microbiol Biotechnol* 74(1):239–243. <https://doi.org/10.1007/s00253-006-0658-1>
- Joseph S, Mathew B (2015a) Microwave-assisted green synthesis of silver nanoparticles and the study on catalytic activity in the degradation of dyes. *J Mol Liq* 204:184–191. <https://doi.org/10.1016/j.molliq.2015.01.027>
- Joseph S, Mathew B (2015b) Microwave assisted facile green synthesis of silver and gold nanocatalysts using the leaf extract of *Aervalanata*. *Spectrochim Acta Part A Mol Biomol Spectrosc* 136:1371–1379. <https://doi.org/10.1016/j.saa.2014.10.023>
- Joseph S, Mathew B (2015c) Facile synthesis of silver nanoparticles and their application in dye degradation. *Mater Sci Eng B* 195:90–97. <https://doi.org/10.1016/j.mseb.2015.02.007>
- Kahrilas GA et al (2013) Microwave-assisted green synthesis of silver nanoparticles using orange peel extract. *ACS Sustain Chem Eng* 2(3):367–376. <https://doi.org/10.1021/sc4003664>
- Kajani AA et al (2014) Green synthesis of anisotropic silver nanoparticles with potent anticancer activity using *Taxusbaccata* extract. *RSC Adv* 4(106):61394–61403. <https://doi.org/10.1039/c4ra08758e>
- Karthik CS et al (2018) Synthesis of novel benzodioxane midst piperazine moiety decorated chitosan silver nanoparticle against biohazard pathogens and as potential anti-inflammatory candidate: a molecular docking studies. *Int J Biol Macromol* 108:489–502. <https://doi.org/10.1016/j.ijbiomac.2017.12.045>
- Koduru JR et al (2018) Phytochemical-assisted synthetic approaches for silver nanoparticles antimicrobial applications: a review. *Adv Colloid Interface Sci* 256:326–339. <https://doi.org/10.1016/j.cis.2018.03.001>
- Kubackova J et al (2014) Sensitive surface-enhanced Raman spectroscopy (SERS) detection of organochlorine pesticides by alkyl dithiol-functionalized metal nanoparticles-induced plasmonic hot spots. *Anal Chem* 87(1):663–669. <https://doi.org/10.1021/ac503672f>
- Kumar R, Kumar G, Umar A (2014) Zinc oxide nanomaterials for photocatalytic degradation of methyl orange: a review. *Nanosci Nanotechnol Lett* 6(8):631–650. <https://doi.org/10.1166/nml.2014.1879>
- Mahakham W et al (2017) Nanoprimering technology for enhancing germination and starch metabolism of aged rice seeds using phyto-synthesized silver nanoparticles. *Sci Rep*. <https://doi.org/10.1038/s41598-017-08669-5>
- Makwana BA et al (2017) A comparative study: metal nanoparticles as fluorescent sensors for biomolecules and their biomedical application. *Sens Actuators B Chem* 246:686–695. <https://doi.org/10.1016/j.snb.2017.02.054>
- Mallikarjuna K et al (2014) Phytochemical fabrication and characterization of silver nanoparticles by using pepper leaf broth. *Arab J Chem* 7(6):1099–1103. <https://doi.org/10.1016/j.arabj.2012.04.001>
- Manikandan R et al (2017) Biosynthesis of silver nanoparticles using aqueous extract of *Phyllanthusacidus* L. fruits and characterization of its anti-inflammatory effect against H<sub>2</sub>O<sub>2</sub> exposed rat peritoneal macrophages. *Process Biochem* 55:172–181. <https://doi.org/10.1016/j.procbio.2017.01.023>
- Mathur N, Bhatnagar P, Verma H (2006) Genotoxicity of vegetables irrigated by industrial wastewater. *J Environ Sci* 18(5):964–968. [https://doi.org/10.1016/s1001-0742\(06\)60022-3](https://doi.org/10.1016/s1001-0742(06)60022-3)
- Mittal A et al (2007) Studies on the adsorption kinetics and isotherms for the removal and recovery of methyl orange from wastewaters using waste materials. *J Hazard Mater* 148(1–2):229–240. <https://doi.org/10.1016/j.jhazmat.2007.02.028>
- Moldovan B et al (2017) In vitro and in vivo anti-inflammatory properties of green synthesized silver nanoparticles using *Viburnum opulus* L. fruits extract. *Mater Sci Eng C* 79:720–727. <https://doi.org/10.1016/j.msec.2017.05.122>



- Ocosy I et al (2018) Biomolecules incorporated metallic nanoparticles synthesis and their biomedical applications. *Mater Lett* 212:45–50. <https://doi.org/10.1016/j.matlet.2017.10.068>
- Ojha S, Sett A, Bora U (2017) Green synthesis of silver nanoparticles by *Ricinus communis* var. *carmencita* leaf extract and its antibacterial study. *Adv Nat Sci Nanosci Nanotechnol* 8(3):035009. <https://doi.org/10.1088/2043-6254/aa724b>
- Ovais M et al (2017) Current state and prospects of the phytosynthesized colloidal gold nanoparticles and their applications in cancer theranostics. *Appl Microbiol Biotechnol* 101(9):3551–3565. <https://doi.org/10.1007/s00253-017-8250-4>
- Park MVDZ et al (2011) The effect of particle size on the cytotoxicity, inflammation, developmental toxicity and genotoxicity of silver nanoparticles. *Biomaterials* 32(36):9810–9817. <https://doi.org/10.1016/j.biomaterials.2011.08.085>
- Paschin YV, Bakhitova LM (1985) Mutagenic effects of thiram in mammalian somatic cells. *Food Chem Toxicol* 23(3):373–375. [https://doi.org/10.1016/0278-6915\(85\)90074-2](https://doi.org/10.1016/0278-6915(85)90074-2)
- Perreault F, Fonseca de Faria A, Elimelech M (2015) Environmental applications of graphene-based nanomaterials. *Chem Soc Rev* 44(16):5861–5896. <https://doi.org/10.1039/c5cs00021a>
- Potara M, Gabudean A-M, Astilean S (2011) Solution-phase, dual LSPR-SERS plasmonic sensors of high sensitivity and stability based on chitosan-coated anisotropic silver nanoparticles. *J Mater Chem* 21(11):3625. <https://doi.org/10.1039/c0jm03329d>
- Priyadarshini E, Pradhan N (2017) Gold nanoparticles as efficient sensors in colorimetric detection of toxic metal ions: a review. *Sens Actuators B Chem* 238:888–902. <https://doi.org/10.1016/j.snb.2016.06.081>
- Rafatullah M et al (2010) Adsorption of methylene blue on low-cost adsorbents: a review. *J Hazard Mater* 177(1–3):70–80. <https://doi.org/10.1016/j.jhazmat.2009.12.047>
- Rafique M et al (2016) A review on green synthesis of silver nanoparticles and their applications. *Artif Cells Nanomed Biotechnol* 45(7):1272–1291. <https://doi.org/10.1080/21691401.2016.1241792>
- Raja S, Ramesh V, Thivaharan V (2017) Green biosynthesis of silver nanoparticles using *Calliandra haematocephala* leaf extract, their antibacterial activity and hydrogen peroxide sensing capability. *Arab J Chem* 10(2):253–261. <https://doi.org/10.1016/j.arabj.2015.06.023>
- Rajaguru P et al (2003) Genotoxicity of a polluted river system measured using the alkaline comet assay on fish and earthworm tissues. *Environ Mol Mutagen* 41(2):85–91. <https://doi.org/10.1002/em.10134>
- Rohit JV, Kailasa SK (2014) Cyclendithiocarbamate-functionalized silver nanoparticles as a probe for colorimetric sensing of thiram and paraquat pesticides via host-guest chemistry. *J Nanopart Res*. <https://doi.org/10.1007/s11051-014-2585-x>
- Rouabhi R (2010) Introduction and toxicology of fungicides. *Fungicides*. <https://doi.org/10.5772/12967>
- Santhosh C et al (2016) Role of nanomaterials in water treatment applications: a review. *Chem Eng J* 306:1116–1137. <https://doi.org/10.1016/j.cej.2016.08.053>
- Saratale RG et al (2017) New insights on the green synthesis of metallic nanoparticles using plant and waste biomaterials: current knowledge, their agricultural and environmental applications. *Environ Sci Pollut Res* 25(11):10164–10183. <https://doi.org/10.1007/s11356-017-9912-6>
- Sebastian M, Aravind A, Mathew B (2018) Green silver-nanoparticle-based dual sensor for toxic Hg(II) ions. *Nanotechnology* 29(35):355502. <https://doi.org/10.1088/1361-6528/aac9a>
- Sebastian M, Aravind A, Mathew B (2019) Green silver nanoparticles based multi-technique sensor for environmental hazardous Cu(II) ion. *BioNanoScience*. <https://doi.org/10.1007/s12668-019-0608-x>
- Shaidarova LG, Budnikov GK, Zaripova SA (2001) Electro-catalytic determination of dithiocarbamate-based pesticides using electrodes modified with metal phthalocyanines. *J Anal Chem* 56(8):748–753. <https://doi.org/10.1023/a:1016741828696>
- Sharma VK, Aulakh JS, Malik AK (2003) Thiram: degradation, applications and analytical methods. *J Environ Monit* 5(5):717. <https://doi.org/10.1039/b304710e>
- Sharma V, Aulakh J, Malik A (2005) Fourth derivative spectrophotometric determination of fungicide thiram (tetramethyldithiocarbamate) using sodium molybdate and its application. *Talanta* 65(2):375–379. <https://doi.org/10.1016/j.talanta.2004.07.001>
- Sharma VK, Yngard RA, Lin Y (2009) Silver nanoparticles: green synthesis and their antimicrobial activities. *Adv Colloid Interface Sci* 145(1–2):83–96. <https://doi.org/10.1016/j.cis.2008.09.002>
- Shrivastava K et al (2016) Localized surface plasmon resonance of silver nanoparticles for sensitive colorimetric detection of chromium in surface water, industrial wastewater and vegetable samples. *Anal Methods* 8(9):2088–2096. <https://doi.org/10.1039/c5ay03120f>
- Shukla A (2014) Facile synthesis of silver nanoparticle and their potential application. *Am J Nanosci Nanotechnol* 2(4):84. <https://doi.org/10.11648/j.nano.20140204.14>
- Silva Junior RC et al (2014) Determination of tetramethylthiuramdisulfide (thiram) for residual analysis in food using spectrophotometry coupled with a solid-phase reactor (SPR) in a flow system. *Int J Environ Anal Chem* 94(9):874–883. <https://doi.org/10.1080/03067319.2014.914183>
- Singh RL, Singh PK, Singh RP (2015) Enzymatic decolorization and degradation of azo dyes—a review. *Int Biodeterior Biodegrad* 104:21–31. <https://doi.org/10.1016/j.ibiod.2015.04.027>
- Singh P et al (2017) In vitro anti-inflammatory activity of spherical silver nanoparticles and monodisperse hexagonal gold nanoparticles by fruit extract of *Prunus serrulata*: a green synthetic approach. *Artif Cells Nanomed Biotechnol*. <https://doi.org/10.1080/21691401.2017.1408117>
- Slimani S et al (2018) The fungicide thiram may disrupt reproductive cycle of domestic male pigeon (*Columba livia domestica*) subjected to a long photoperiod. *Pak J Zool*. <https://doi.org/10.17582/journal.pjz.2018.50.5.1693.1701>
- Soliveri G et al (2016) Microwave-assisted silver nanoparticle film formation for SERS applications. *J Phys Chem C* 120(2):1237–1244. <https://doi.org/10.1021/acs.jpcc.5b10833>
- Sotiriou GA, Pratsinis SE (2010) Antibacterial activity of nanosilver ions and particles. *Environ Sci Technol* 44(14):5649–5654. <https://doi.org/10.1021/es101072s>
- Stathi P et al (2006) Effects of dissolved carboxylates and carbonates on the adsorption properties of thiuram disulfate pesticides. *Environ Sci Technol* 40(1):221–227. <https://doi.org/10.1021/es051451s>
- Tan KB et al (2015) Adsorption of dyes by nanomaterials: recent developments and adsorption mechanisms. *Sep Purif Technol* 150:229–242. <https://doi.org/10.1016/j.seppur.2015.07.009>
- Tran QH, Nguyen VQ, Le A-T (2013) Silver nanoparticles: synthesis, properties, toxicology, applications, and perspectives. *Adv Nat Sci Nanosci Nanotechnol* 4(3):033001. <https://doi.org/10.1088/2043-6262/4/3/033001>
- Tushar KV et al (2008) *Coscium fenestratum* (Gaertn.) Colebr.—a review on this rare, critically endangered and highly-traded medicinal species. *J Plant Sci* 3(2):133–145. <https://doi.org/10.3923/jps.2008.133.145>
- Veisi H, Azizi S, Mohammadi P (2018) Green synthesis of the silver nanoparticles mediated by *Thymbraspicata* extract and its application as a heterogeneous and recyclable nanocatalyst for catalytic reduction of a variety of dyes in water. *J Clean Prod* 170:1536–1543. <https://doi.org/10.1016/j.jclepro.2017.09.265>
- Vijayan R, Joseph S, Mathew B (2017a) Indigoferatinctoria leaf extract mediated green synthesis of silver and gold nanoparticles and



- assessment of their anticancer, antimicrobial, antioxidant and catalytic properties. *Artif Cells Nanomed Biotechnol* 46(4):861–871. <https://doi.org/10.1080/21691401.2017.1345930>
- Vijayan R, Joseph S, Mathew B (2017b) Green synthesis, characterization and applications of noble metal nanoparticles using *Myxopyrum serratum* A. W. Hill leaf extract. *BioNanoScience* 8(1):105–117. <https://doi.org/10.1007/s12668-017-0433-z>
- Vijayaraghavan K, Ashokkumar T (2017) Plant-mediated biosynthesis of metallic nanoparticles: a review of literature, factors affecting synthesis, characterization techniques and applications. *J Environ Chem Eng* 5(5):4866–4883. <https://doi.org/10.1016/j.jece.2017.09.026>
- Wan D et al (2009) One-shot deep-UV pulsed-laser-induced photomodification of hollow metal nanoparticles for high-density data storage on flexible substrates. *ACS Nano* 4(1):165–173. <https://doi.org/10.1021/nn9013005>
- Wang Q, Wu D, Chen Z (2015) Ag dendritic nanostructures for rapid detection of thiram based on surface-enhanced Raman scattering. *RSC Adv* 5(86):70553–70557. <https://doi.org/10.1039/c5ra13080h>
- Wu M et al (2017) Removal of silver nanoparticles by mussel-inspired  $\text{Fe}_3\text{O}_4$ @ polydopamine core-shell microspheres and its use as efficient catalyst for methylene blue reduction. *Sci Rep*. <https://doi.org/10.1038/srep42773>
- Yang J-K et al (2014) Single-step and rapid growth of silver nanoshells as SERS-active nanostructures for label-free detection of pesticides. *ACS Appl Mater Interfaces* 6(15):12541–12549. <https://doi.org/10.1021/am502435x>
- Yuan C et al (2011) Single clusters of self-assembled silver nanoparticles for surface-enhanced Raman scattering sensing of a dithiocarbamate fungicide. *J Mater Chem* 21(40):16264. <https://doi.org/10.1039/c1jm12919h>
- Zhang J, Chaker M, Ma D (2017a) Pulsed laser ablation based synthesis of colloidal metal nanoparticles for catalytic applications. *J Colloid Interface Sci* 489:138–149. <https://doi.org/10.1016/j.jcis.2016.07.050>
- Zhang Y et al (2017b) Ultrafine metal nanoparticles/N-doped porous carbon hybrids coated on carbon fibers as flexible and binder-free water splitting catalysts. *Adv Energy Mater* 7(15):1700220. <https://doi.org/10.1002/aenm.201700220>
- Zheng Y et al (2017) Hot luminescence from gold nanoflowers and its application in high-density optical data storage. *Opt Express* 25(8):9262. <https://doi.org/10.1364/oe.25.009262>

